

# **Supporting Information**

## **Conformational Stability of Fibrillar Amyloid-beta Oligomers via Protofilament Pair Formation – A Systematic Computational Study**

Anna Kahler<sup>1</sup>, Heinrich Sticht<sup>1</sup>, Anselm H.C. Horn<sup>1,\*</sup>

**1 Bioinformatik, Institut für Biochemie, Friedrich-Alexander-Universität Erlangen-Nürnberg, Erlangen, Germany**

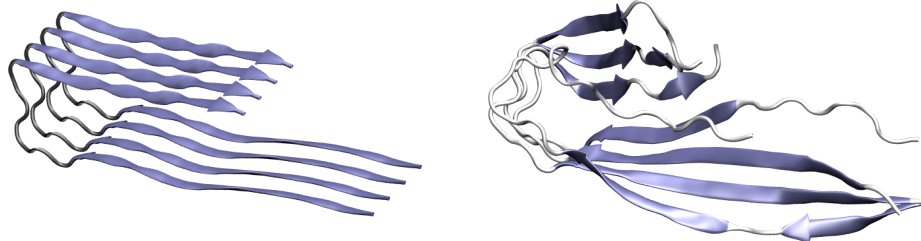
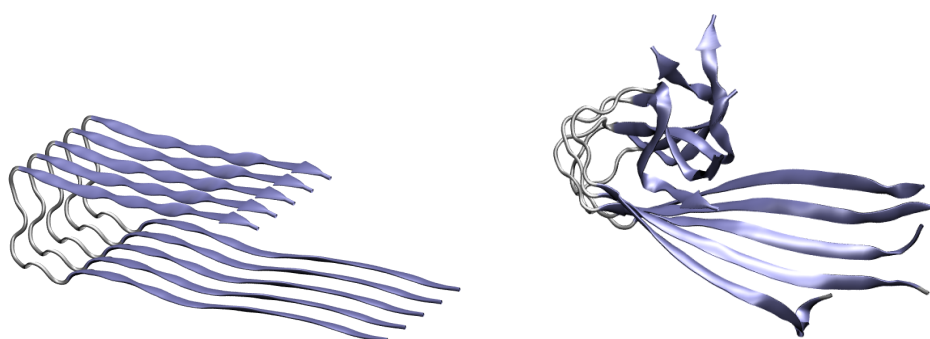
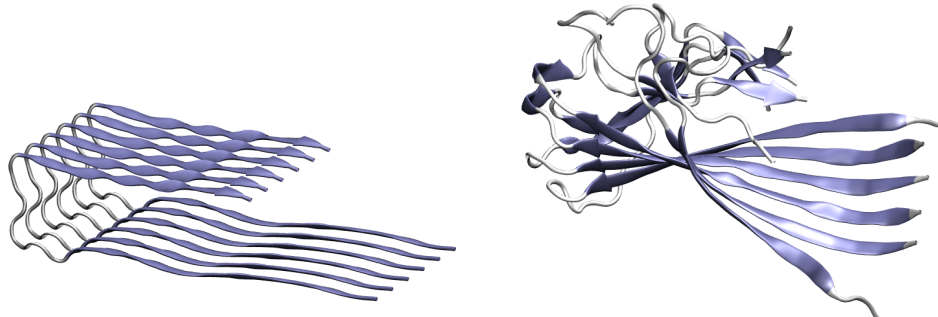
\* E-mail: [anselm.horn@biochem.uni-erlangen.de](mailto:anselm.horn@biochem.uni-erlangen.de)

## List of Figures

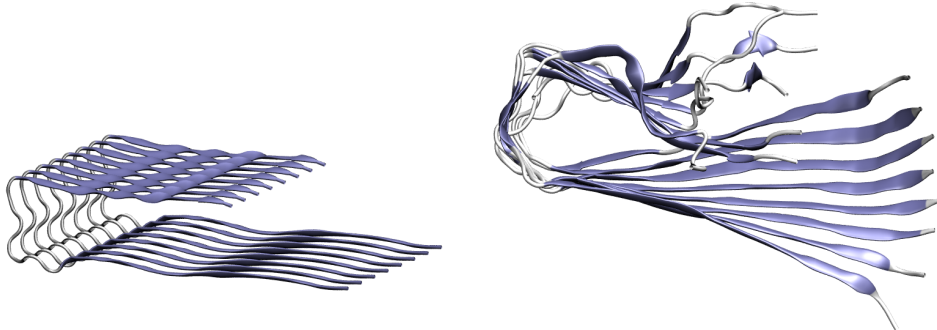
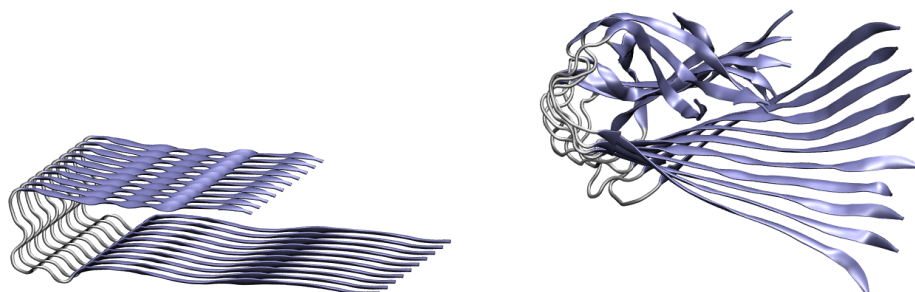
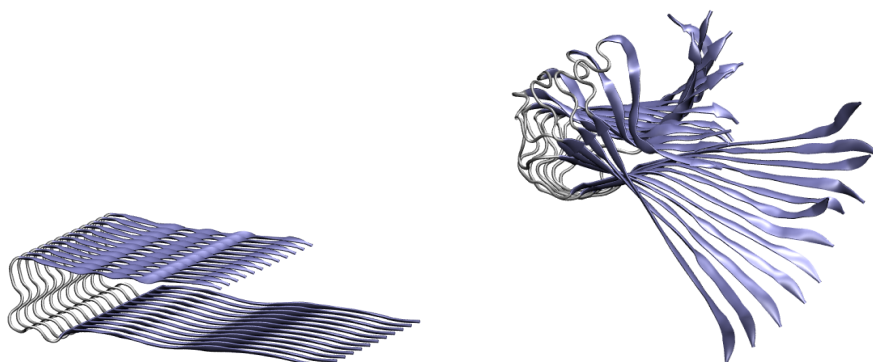
S1	Small protofilaments $O_4$ , $O_5$ , and $O_6$ with their initial structure and the structure after 50 ns of simulation. . . . .	3
S2	Medium-sized protofilaments $O_8$ , $O_{10}$ , and $O_{12}$ with their initial structure and the structure after 50 ns of simulation. . . . .	4
S3	Large protofilaments $O_{24}$ and $O_{48}$ with their initial structure and the structure after 50 ns of simulation. . . . .	5
S4	Tiny protofilament pairs $O_{2 \times 1}$ , $O_{2 \times 2}$ , and $O_{2 \times 3}$ with their initial structure and the structure after 50 ns of simulation. . . . .	6
S5	Small protofilament pairs $O_{2 \times 4}$ , $O_{2 \times 5}$ , and $O_{2 \times 6}$ with their initial structure and the structure after 50 ns of simulation. . . . .	7
S6	Large protofilament pairs $O_{2 \times 12}$ and $O_{2 \times 24}$ with their initial structure and the structure after 50 ns of simulation. . . . .	8
S7	Rmsd values for the simulations of the tiny oligomers, 4-mer, 5-mer, 6-mer, 8-mers, and 10-mers. . . . .	9
S8	Rmsd values for the simulations of the 12-mer, 24-mers, and 48-mers. . . . .	10
S9	Number of hydrogen bonds for the simulations of the tiny oligomers, 4-mer, 5-mer, 6-mer, 8-mers, and 10-mers. . . . .	11
S10	Number of hydrogen bonds for the simulations of the 12-mers, 24-mers, and 48-mers. . . . .	12
S11	Twist angle of the oligomer for the simulations of the 4-mer, the 5-mer, the 6-mer, and the two 8-mers. . . . .	13
S12	Twist angle of the oligomer for the simulations of the 10-mers, 12-mers, 24-mers, and 48-mers. . . . .	14
S13	Content of parallel $\beta$ -sheet for the small oligomers $O_4$ , $O_5$ and $O_6$ . . . . .	15
S14	Content of parallel $\beta$ -sheet for the oligomers $O_8$ and $O_{2 \times 4}$ . . . . .	16
S15	Content of parallel $\beta$ -sheet for the oligomers $O_{10}$ and $O_{2 \times 5}$ . . . . .	17
S16	Content of parallel $\beta$ -sheet for the oligomers $O_{12}$ and $O_{2 \times 6}$ . . . . .	18
S17	Content of parallel $\beta$ -sheet for the large protofilament $O_{24}$ . . . . .	19
S18	Content of parallel $\beta$ -sheet for the large protofilament pair $O_{2 \times 12}$ . . . . .	20
S19	Content of parallel $\beta$ -sheet for the large protofilament $O_{48}$ . . . . .	21
S20	Content of parallel $\beta$ -sheet for the large protofilament $O_{48}$ . . . . .	22
S21	Content of parallel $\beta$ -sheet for the large protofilament pair $O_{2 \times 24}$ . . . . .	23
S22	Content of parallel $\beta$ -sheet for the large protofilament pair $O_{2 \times 24}$ . . . . .	24

## List of Tables

S1	Appearance of inter- and intramolecular salt bridges (in %) in the MD simulation. . . . .	25
----	---	----

**A****B****C**

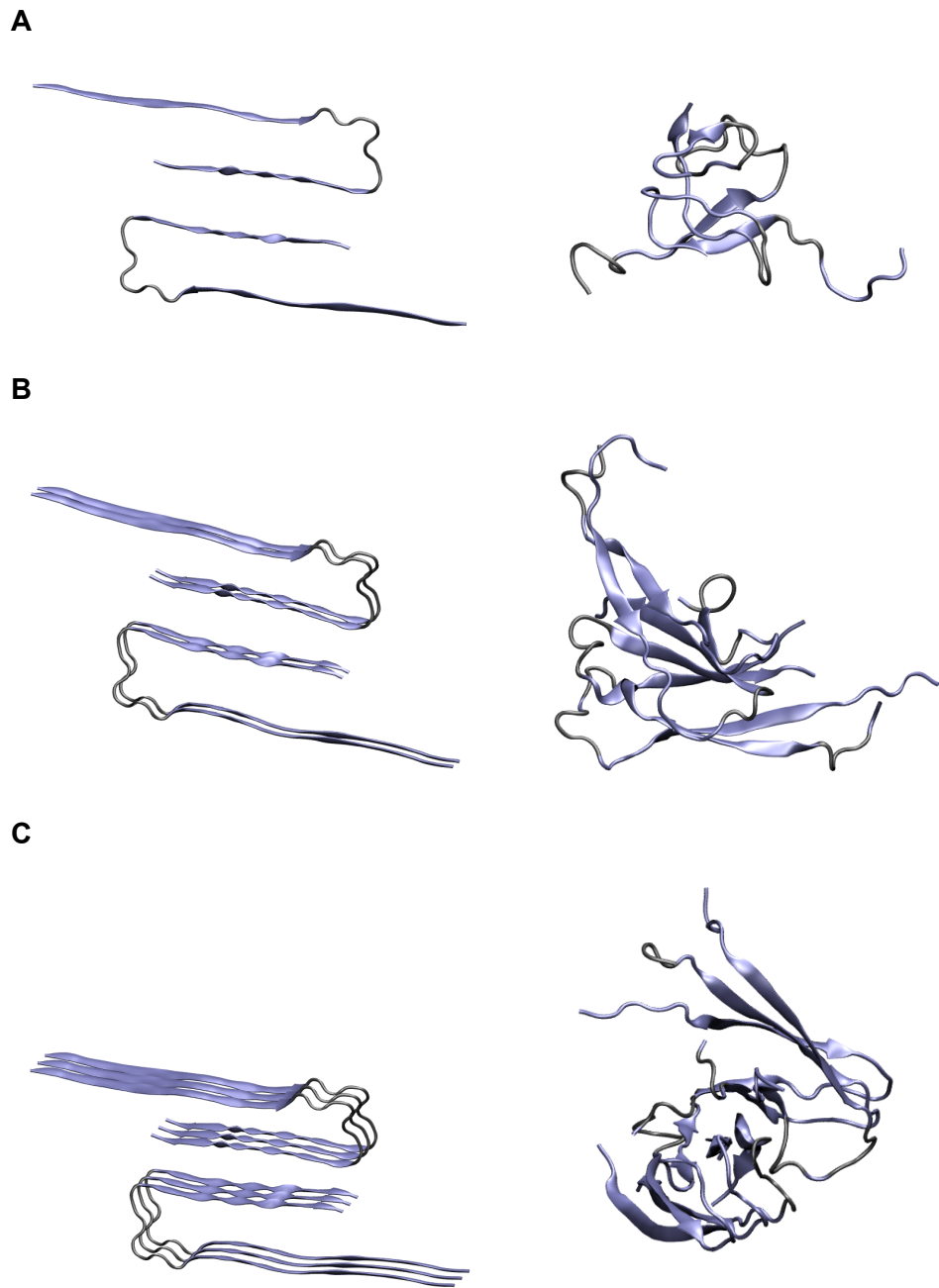
**Figure S1. Small protofilaments O<sub>4</sub>, O<sub>5</sub>, and O<sub>6</sub> with their initial structure and the structure after 50 ns of simulation.** The upper C-terminal chains in O<sub>4</sub> (A) bend upwards to cover the hydrophobic residues pointing towards the solvent. This flexible hinge can also be observed in the other oligomers O<sub>5</sub> and O<sub>6</sub>; in the 5-mer (B) the twisting of parallel  $\beta$ -sheets can already be observed but it is more obvious in the 6-mer (C).

**A****B****C**

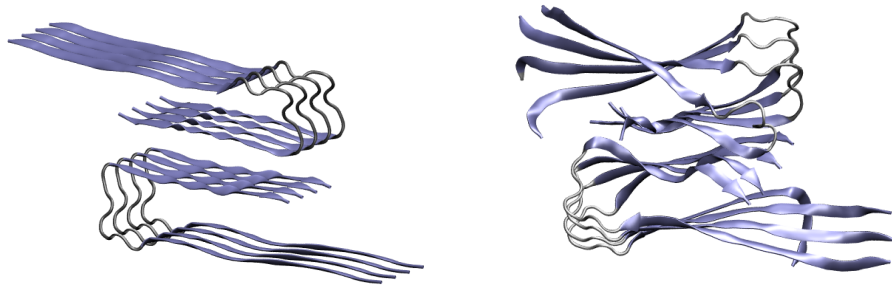
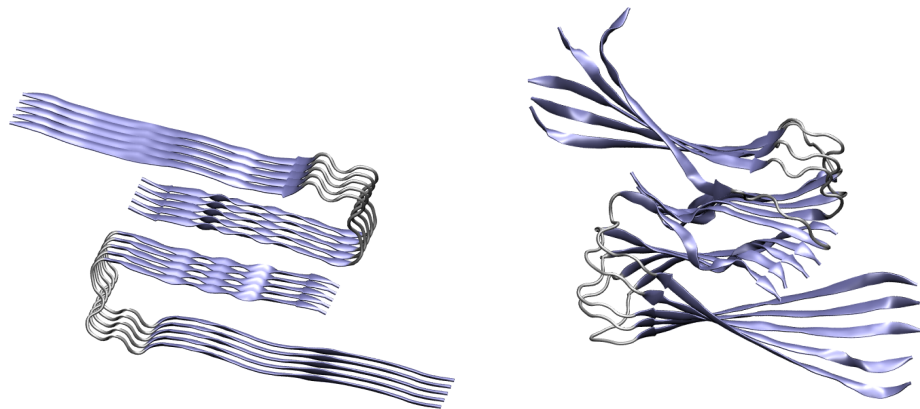
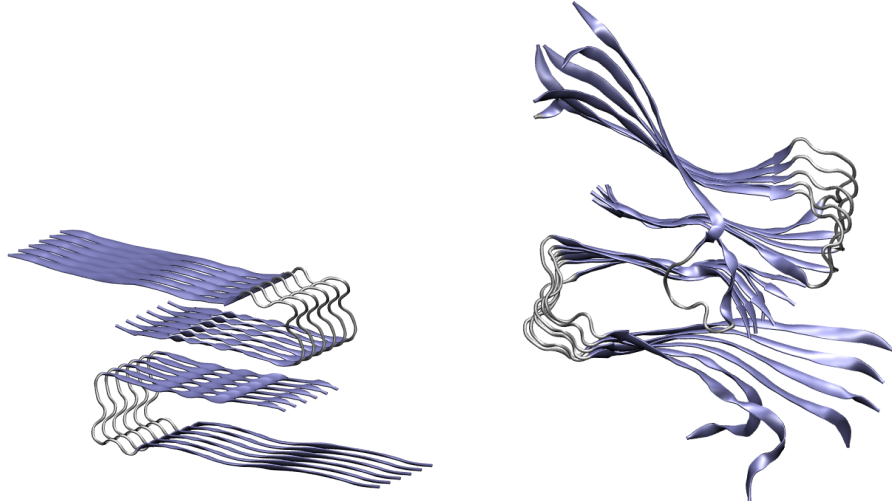
**Figure S2. Medium-sized protofilaments O<sub>8</sub>, O<sub>10</sub>, and O<sub>12</sub> with their initial structure and the structure after 50 ns of simulation.** Twisting of parallel  $\beta$ -sheets is strongly pronounced in oligomers with around 10 monomers. In the 8-mer (A) the flexible hinge is present in all C-terminal chains whereas it is less present in the middle chains of the 10-mer (B) and the 12-mer (C).

**A****B**

**Figure S3. Large protofilaments  $O_{24}$  and  $O_{48}$  with their initial structure and the structure after 50 ns of simulation.** The most obvious structural property in the large oligomers is the extensive twist around the elongation axis. The 24-mer (A) twists about 110° and the 48-mer (B) nearly one way around (335°). The flexible hinge is only present in the C-termini of the outer chains.



**Figure S4.** Tiny protofilament pairs  $O_{2\times 1}$ ,  $O_{2\times 2}$ , and  $O_{2\times 3}$  with their initial structure and the structure after 50 ns of simulation. (A) The protofilament pair dimer completely lost its initial conformation. (B) The protofilament pair tetramer rearranges to hide hydrophobic residues from the solvent. (C) The protofilament pair hexamer keeps the conformation of the trimer parts but rearranges to cover hydrophobic residues.

**A****B****C**

**Figure S5. Small protofilament pairs  $O_{2 \times 4}$ ,  $O_{2 \times 5}$ , and  $O_{2 \times 6}$  with their initial structure and the structure after 50 ns of simulation.** These oligomers exhibit structural properties of their smaller building blocks: the twist angle and the flexible hinge although the latter is not that much present due to the C-terminal contacts. The 8-mer (A) reveals a larger twist than the 12-mer (C) because the larger hydrophobic interface in the 12-mer compensates the twist of parallel  $\beta$ -sheets. The 10-mer (B) combines properties of the other two: a large twist and a medium hydrophobic interface.

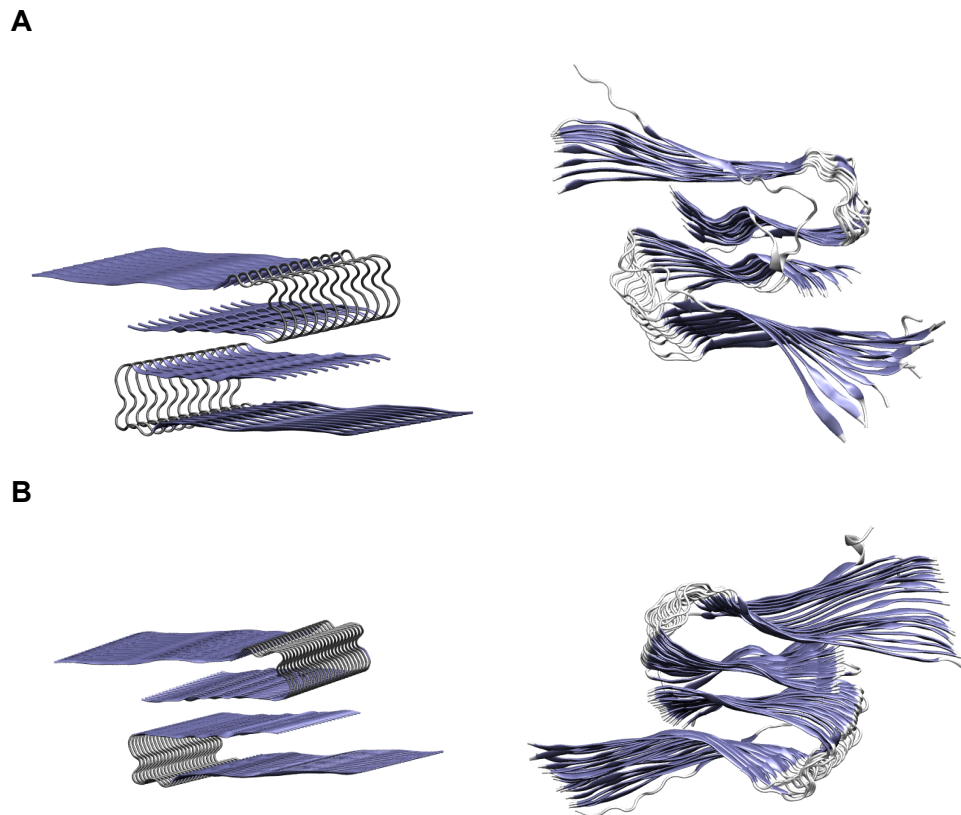


**Figure S6. Large protofilament pairs  $O_{2 \times 12}$  and  $O_{2 \times 24}$  with their initial structure and the structure after 50 ns of simulation.** The hydrophobic interaction via the C-terminal interface diminishes the twisting effect of parallel  $\beta$ -sheets. The 24-mer (A) twists much less than its protofilament counterpart (Figure S3A); the same can be seen for the 48-mer (B) and its protofilament counterpart (Figure S3B).

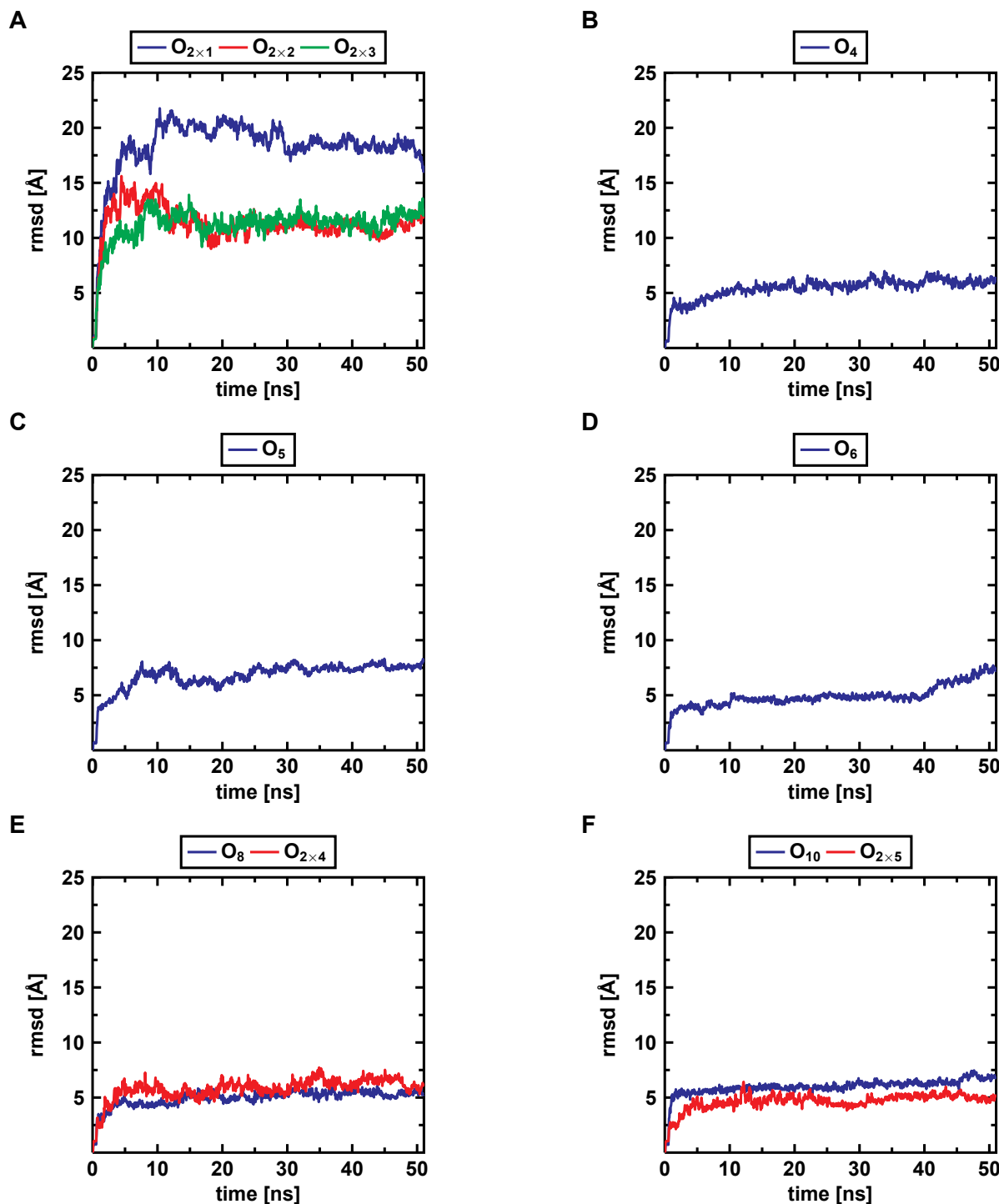


**Figure S7.** Rmsd values for the simulations of the tiny oligomers, 4-mer, 5-mer, 6-mer, 8-mers, and 10-mers. The values of the tiny oligomers' simulations (A) are too large to describe stable simulations. The values of the other simulations (B-F) are in the range for simulations of globular shaped proteins.

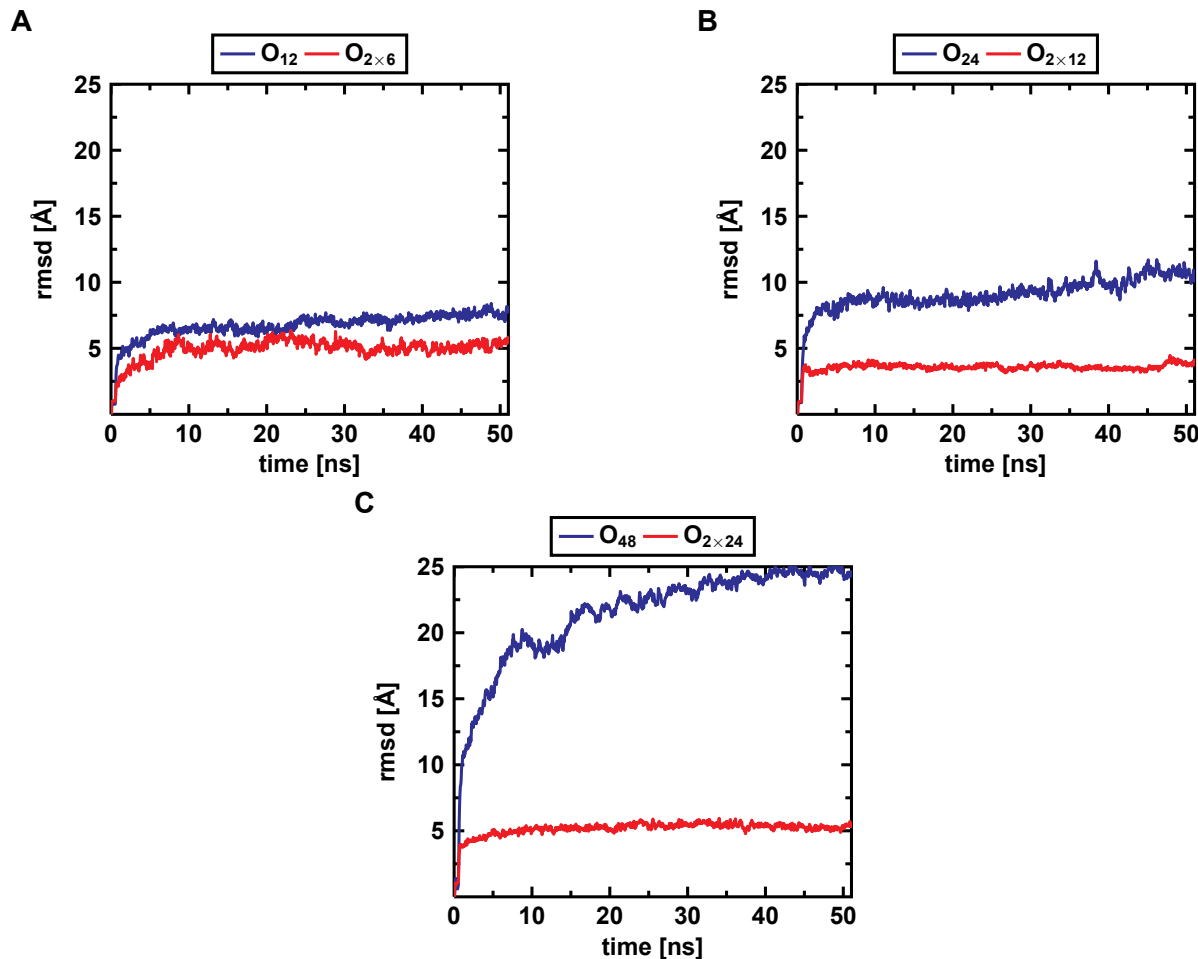


**Figure S8.** Rmsd values for the simulations of the 12-mers, 24-mers, and 48-mers. The rmsd-values of the protofilament pair simulations (red lines in A–C) are in the range for simulations of globular shaped proteins and indicate stable simulations. Increasing values of the protofilaments (blue lines in A–C) suggest either unstable simulations or severe distortions in the system.

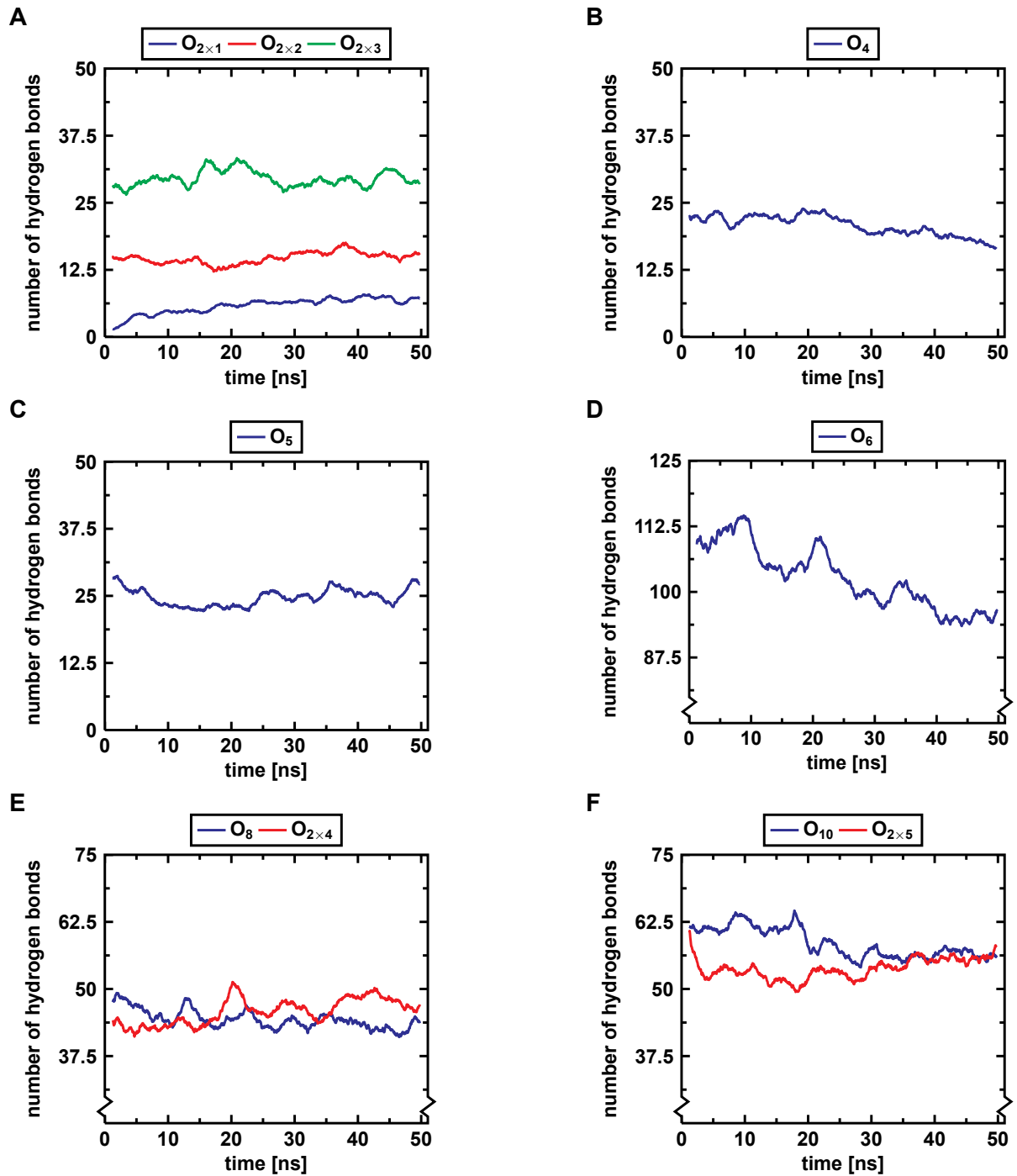


**Figure S9.** Number of hydrogen bonds for the simulations of the tiny oligomers, 4-mer, 5-mer, 6-mer, 8-mers, and 10-mers. (A) The tiny protofilament pairs  $O_{2\times 1}$ ,  $O_{2\times 2}$ , and  $O_{2\times 3}$ . (B) The protofilament tetramer. (C) The protofilament pentamer. (D) The protofilament hexamer. (E) The protofilament and the protofilament pair octamer. (F) The protofilament and the protofilament pair decamer.

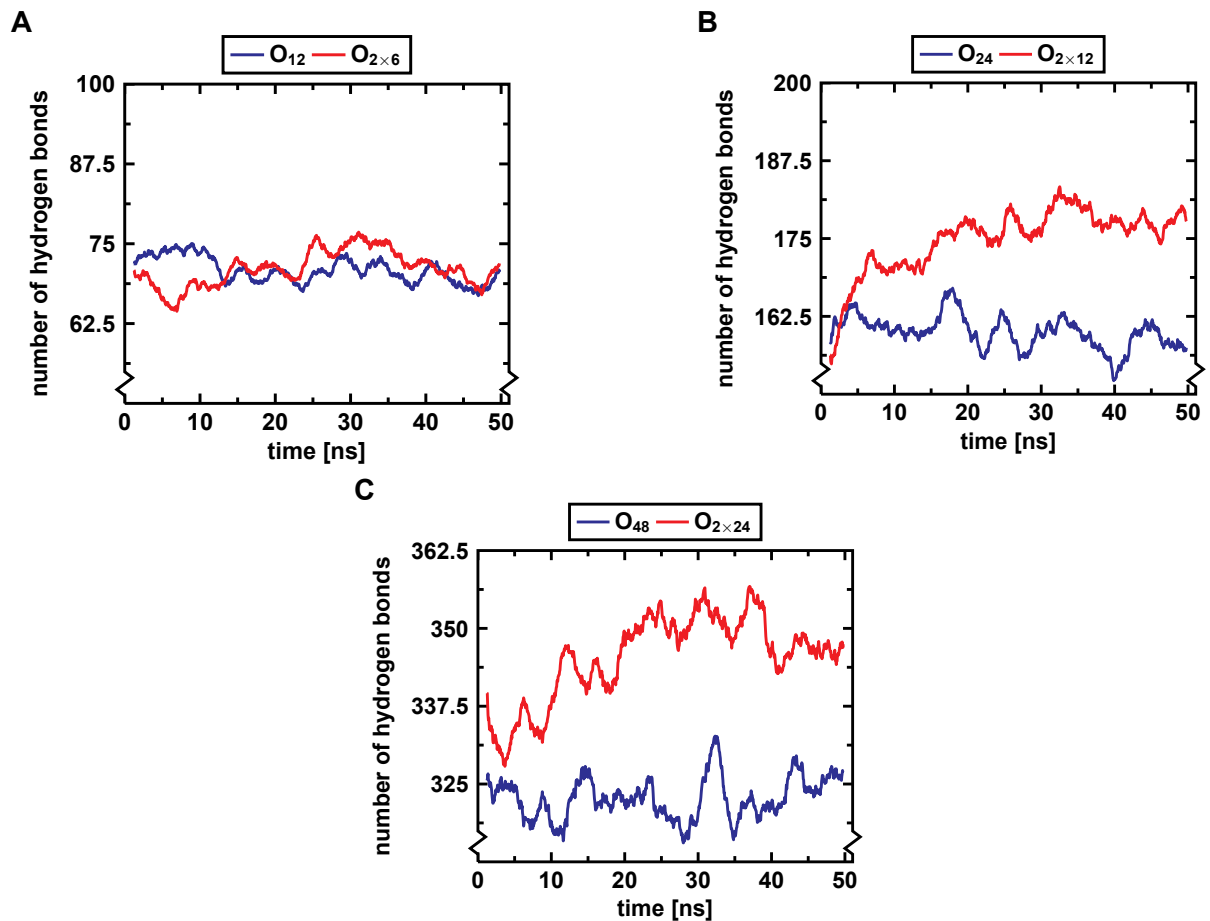


**Figure S10. Number of hydrogen bonds for the simulations of the 12-mers, 24-mers, and 48-mers.** (A) The protofilament and the protofilament pair dodecamer. (B) The protofilament and the protofilament pair 24-mer. (C) The protofilament and the protofilament pair 48-mer.

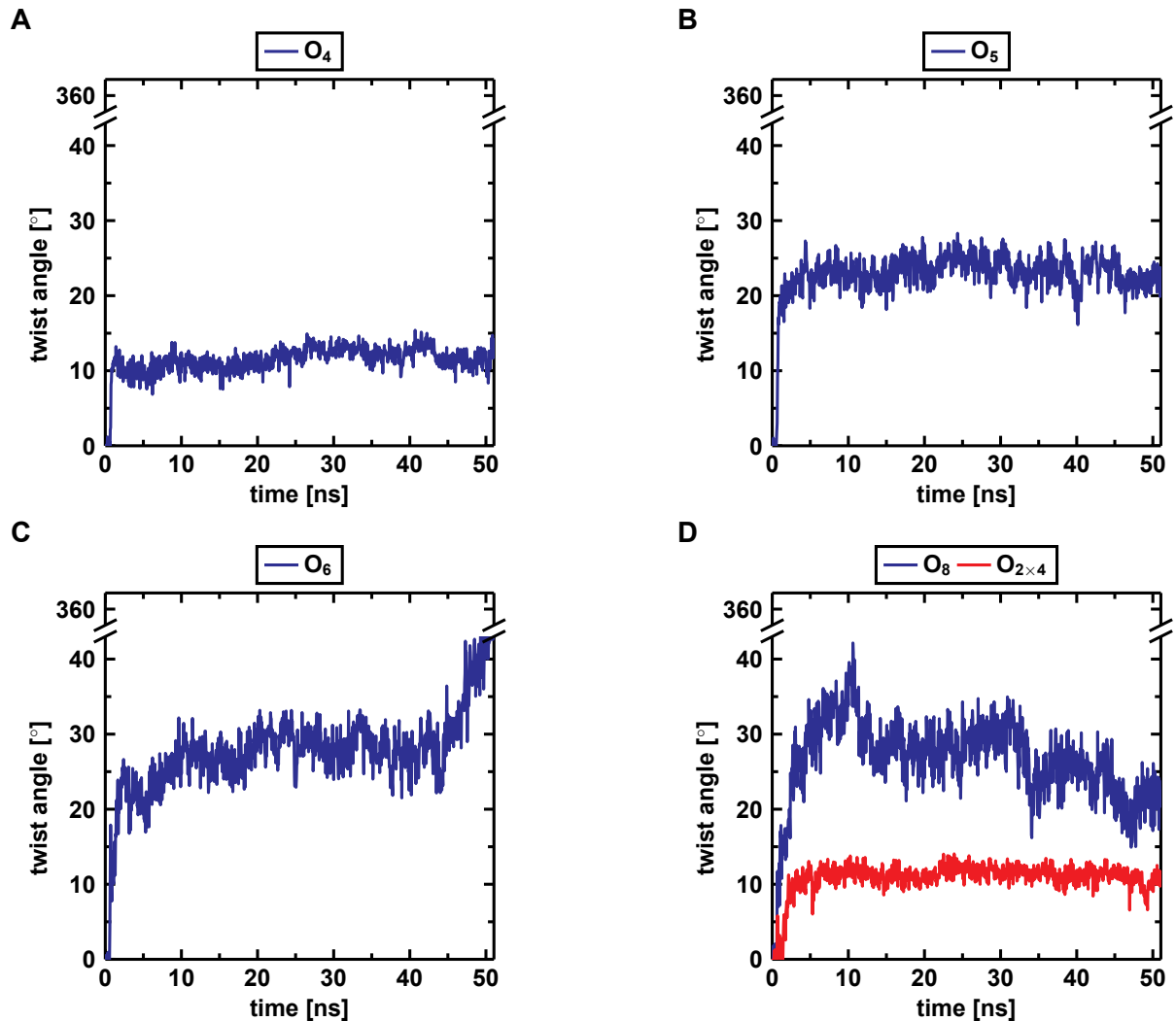


**Figure S11. Twist angle of the oligomer for the simulations of the 4-mer, the 5-mer, the 6-mer, and the two 8-mers.** (A) The twist angle for the protofilament tetramer. (B) The twist angle for the protofilament pentamer. (C) The twist angle for the protofilament hexamer. (D) The twist angles for the protofilament and the protofilament pair octamers.

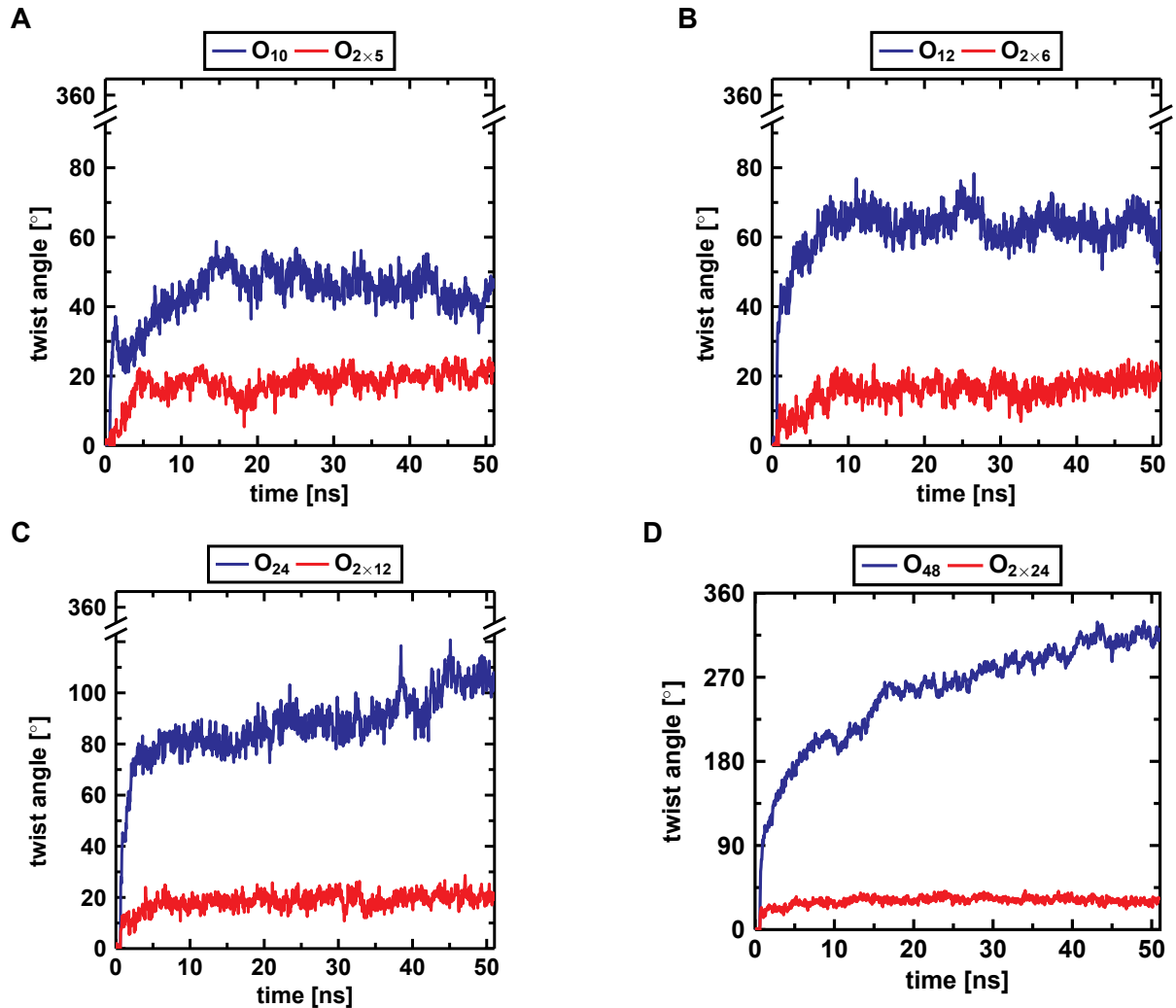


**Figure S12. Twist angle of the oligomer for the simulations of the 10-mers, 12-mers, 24-mers, and 48-mers.** (A) The twist angles for the protofilament and the protofilament pair 10-mers. (B) The twist angles for the protofilament and the protofilament pair 12-mers. (C) The twist angles for the protofilament and the protofilament pair 24-mers. (D) The twist angles for the protofilament and the protofilament pair 48-mers.

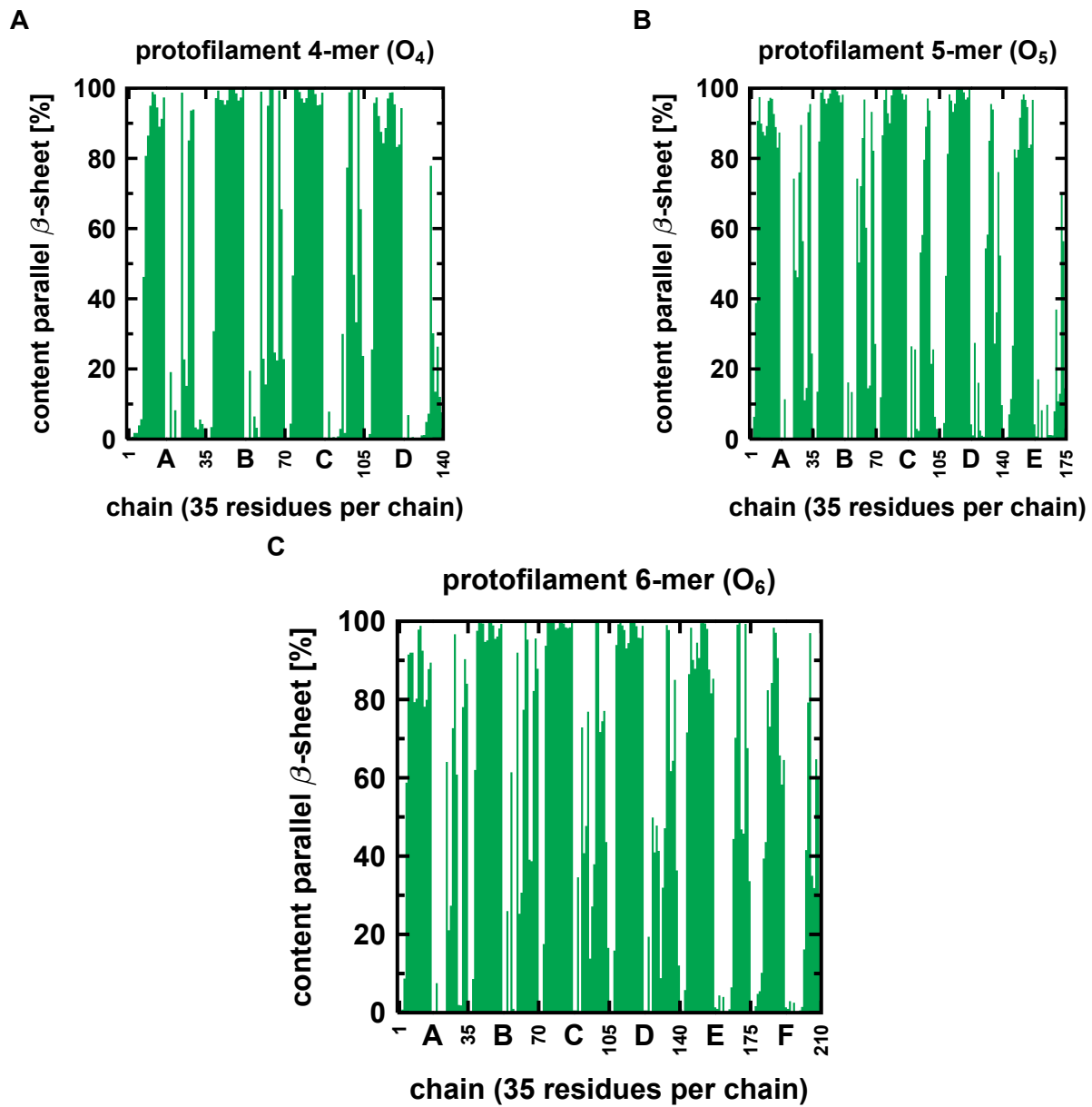


**Figure S13.** Content of parallel  $\beta$ -sheet for the small oligomers  $O_4$ ,  $O_5$  and  $O_6$ . (A) The protofilament tetramer. (B) The protofilament pentamer. (C) The protofilament hexamer.

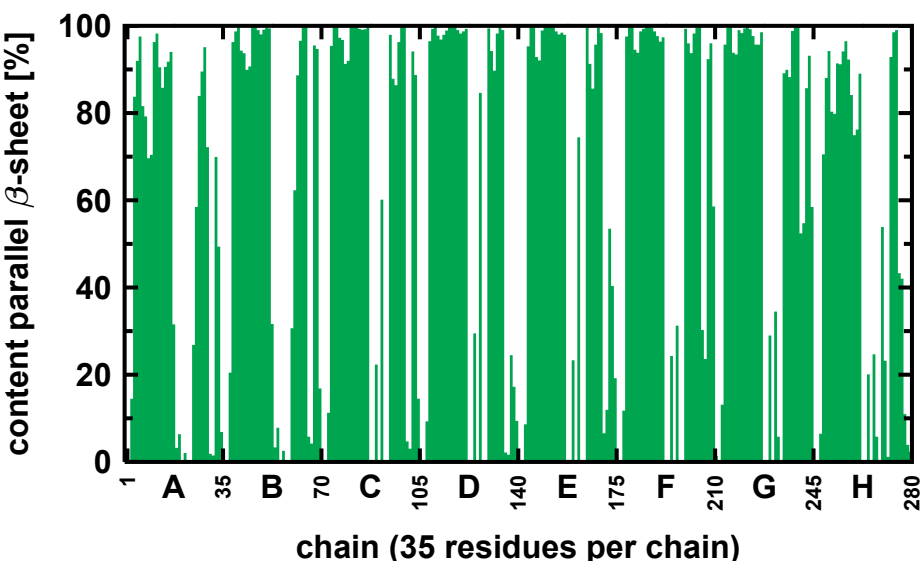
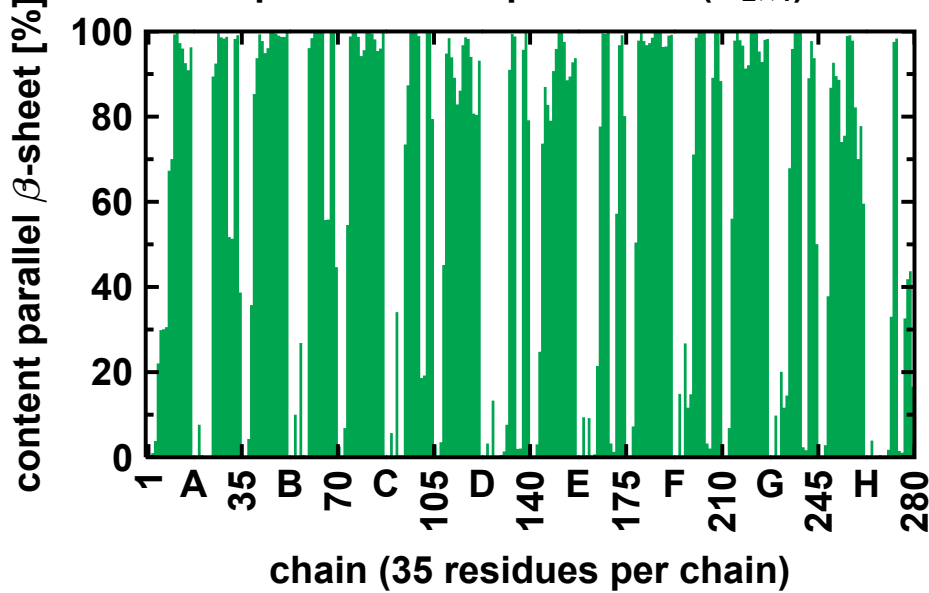
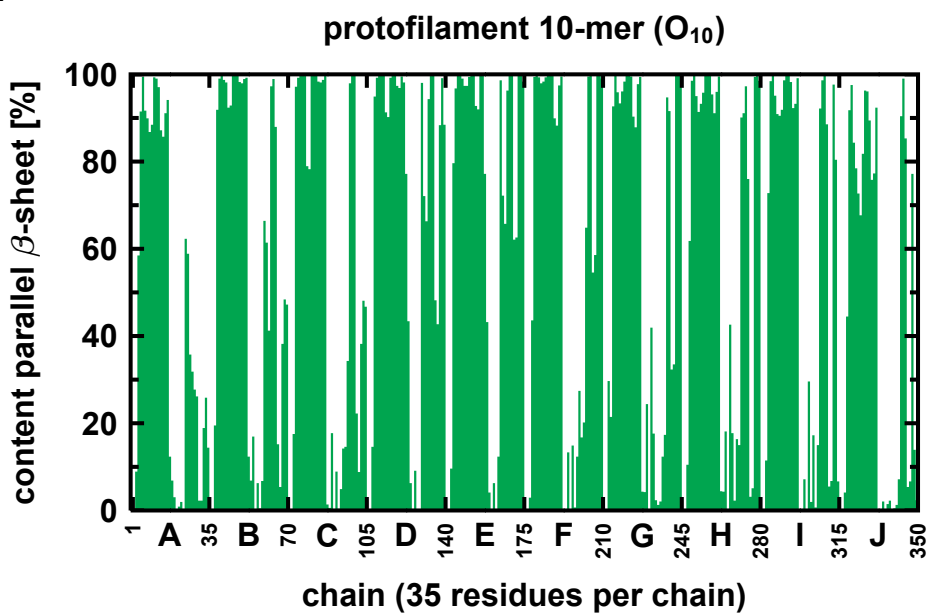
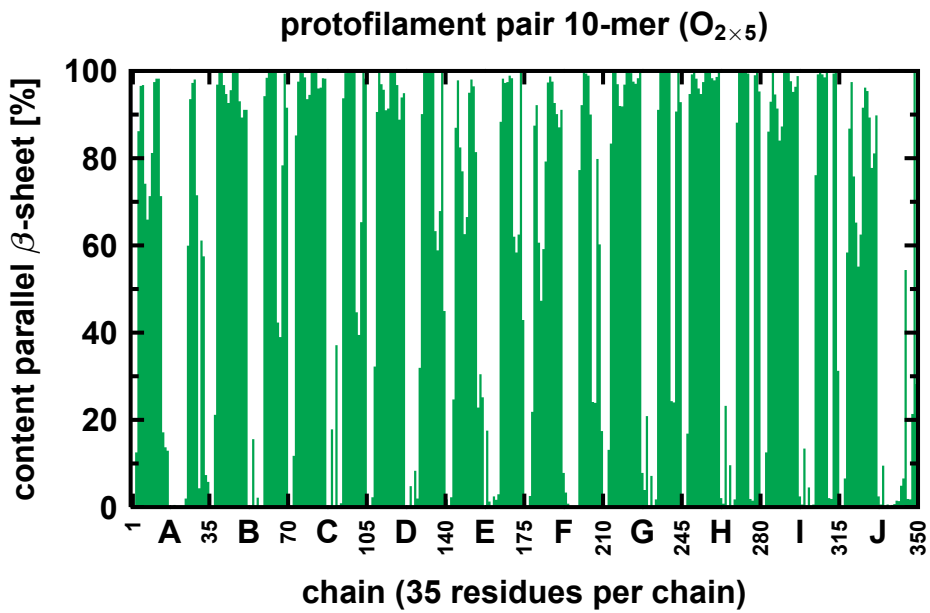
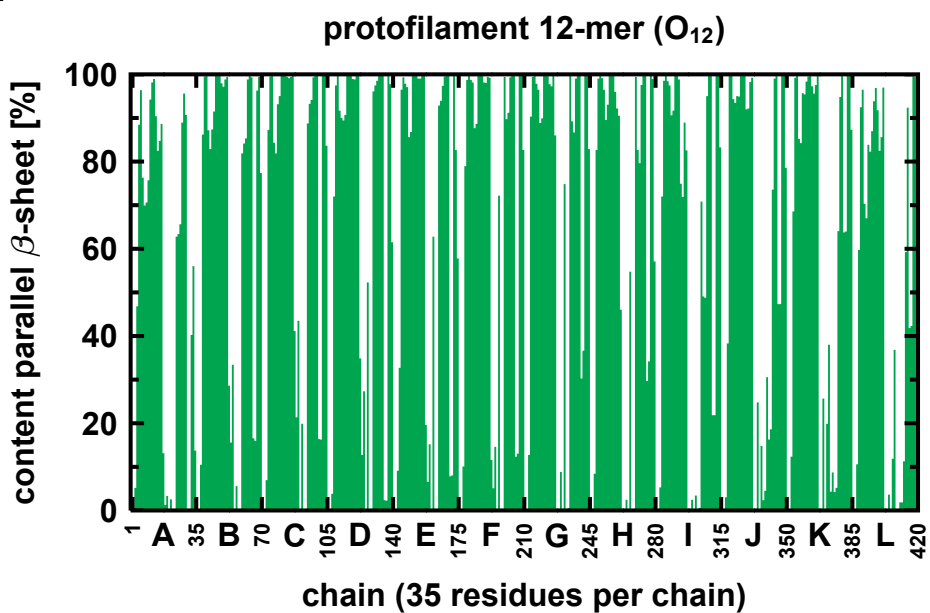
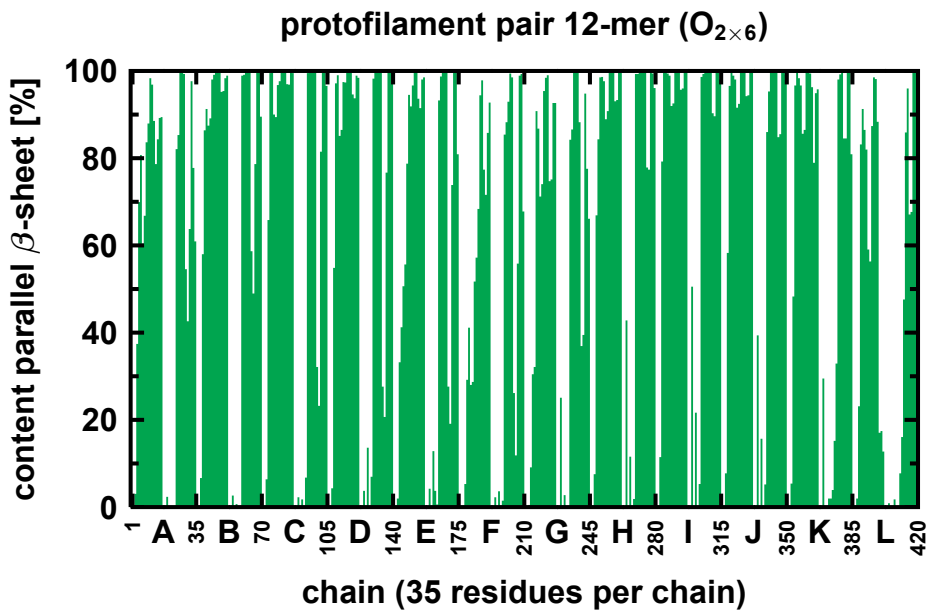
**A**protofilament 8-mer ( $O_8$ )**B**protofilament pair 8-mer ( $O_{2 \times 4}$ )

Figure S14. Content of parallel  $\beta$ -sheet for the oligomers  $O_8$  and  $O_{2 \times 4}$ . (A) The protofilament octamer. (B) The protofilament pair octamer.

**A****B**

**Figure S15.** Content of parallel  $\beta$ -sheet for the oligomers  $O_{10}$  and  $O_{2 \times 5}$ . (A) The protofilament decamer. (B) The protofilament pair decamer.

**A****B**

**Figure S16.** Content of parallel  $\beta$ -sheet for the oligomers  $O_{12}$  and  $O_{2 \times 6}$ . (A) The protofilament dodecamer. (B) The protofilament pair dodecamer.

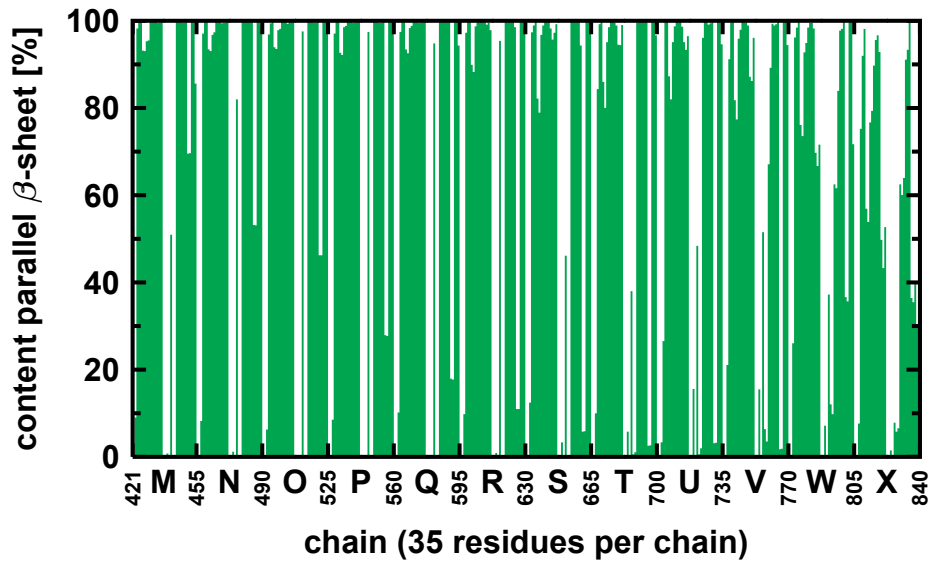
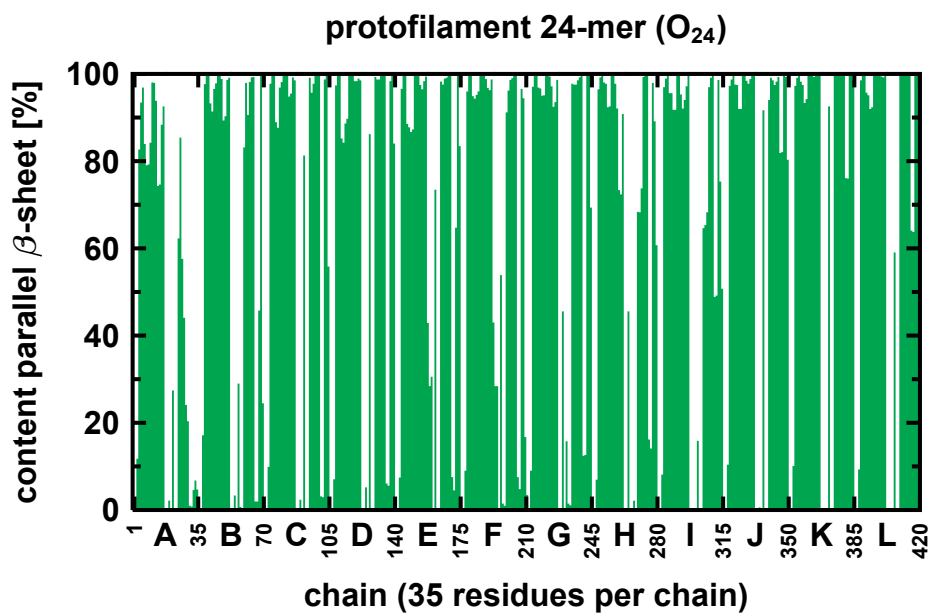


Figure S17. Content of parallel  $\beta$ -sheet for the large protofilament  $O_{24}$ .

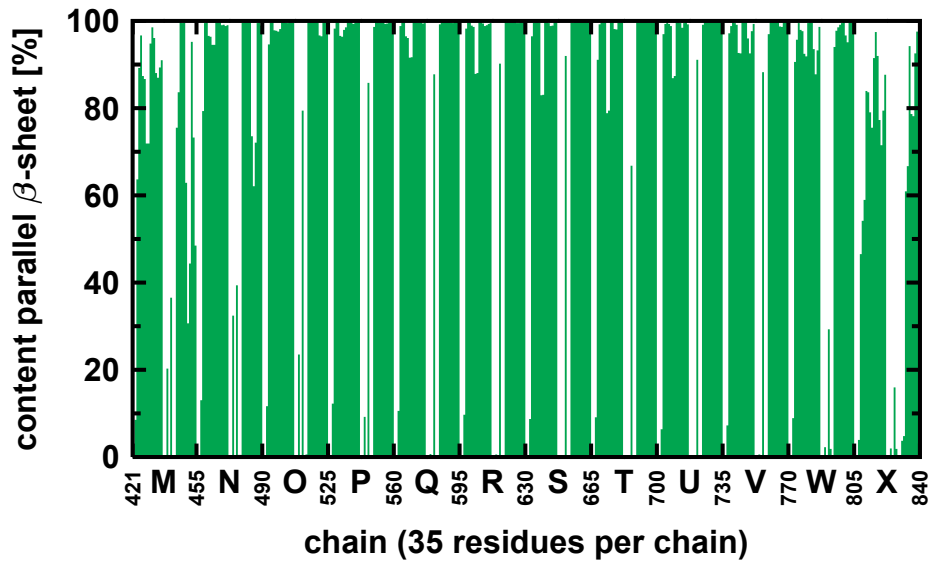
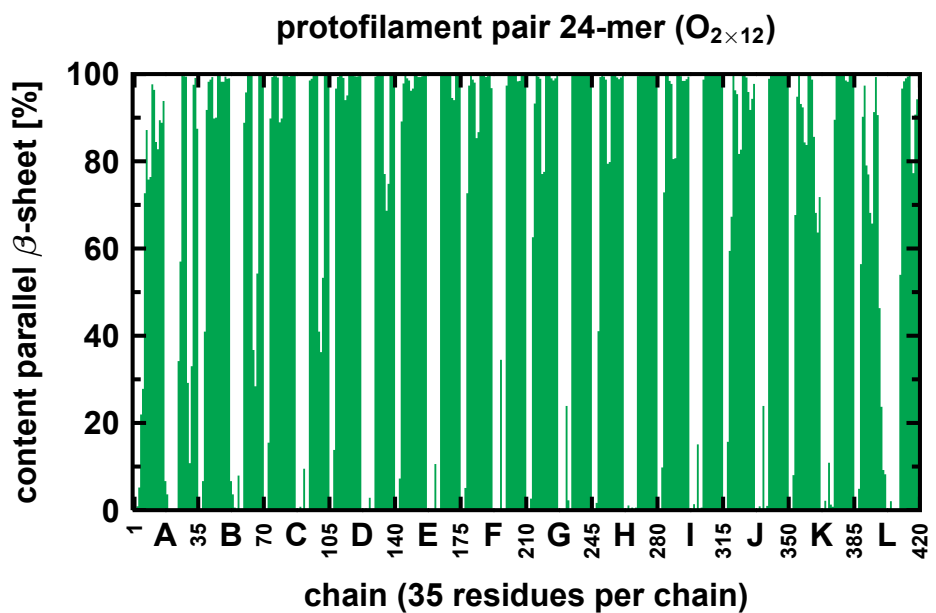
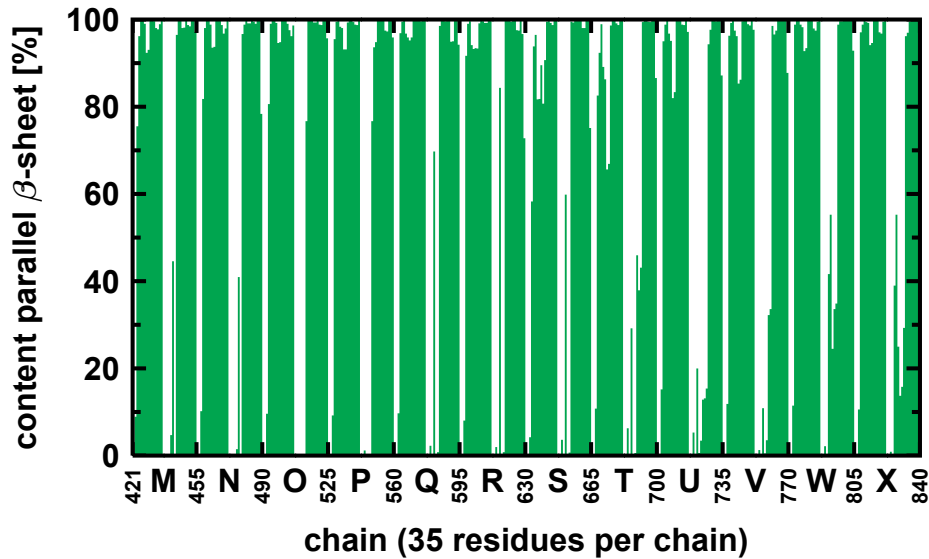
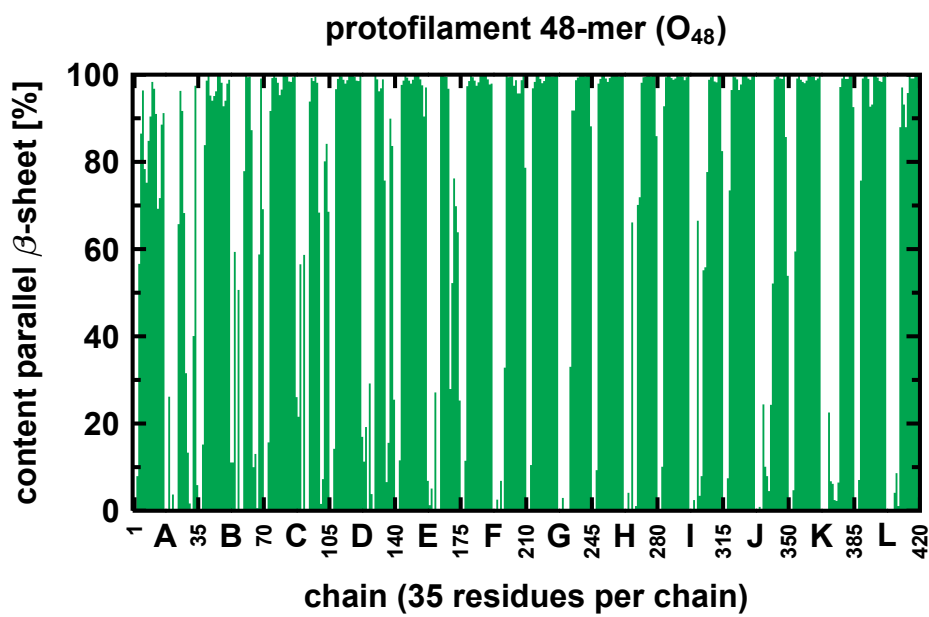
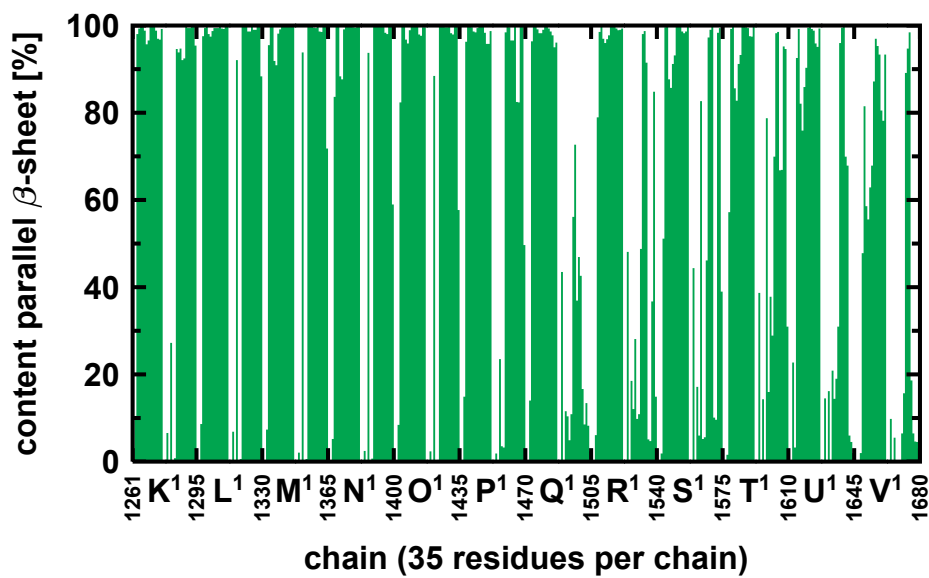
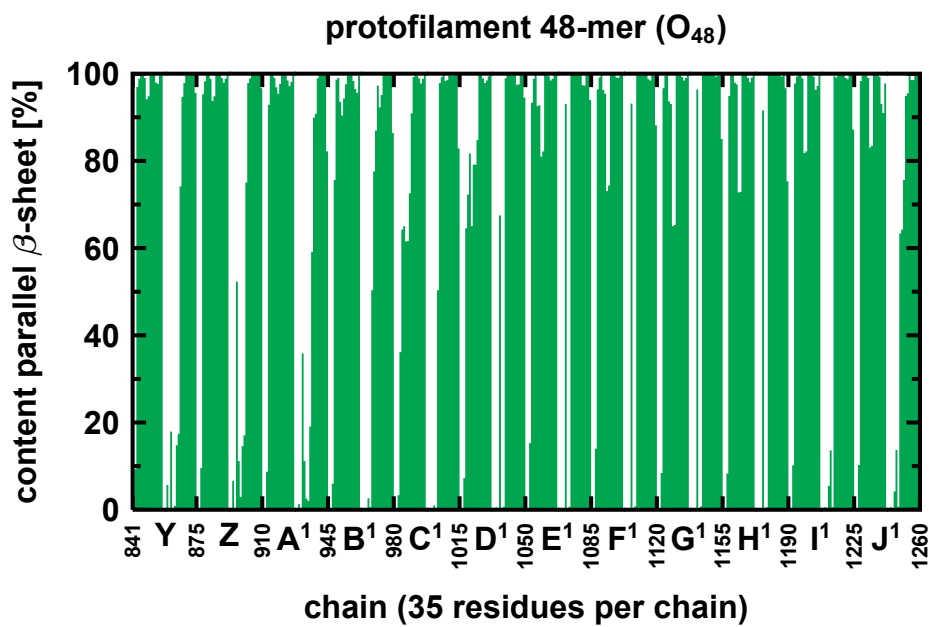


Figure S18. Content of parallel  $\beta$ -sheet for the large protofilament pair  $O_{2 \times 12}$ .



**Figure S19.** Content of parallel  $\beta$ -sheet for the large protofilament  $O_{48}$ . Depicted are the first 24  $A\beta$  chains.



**Figure S20.** Content of parallel  $\beta$ -sheet for the large protofilament  $O_{48}$ . Depicted are the last 24 A $\beta$  chains.

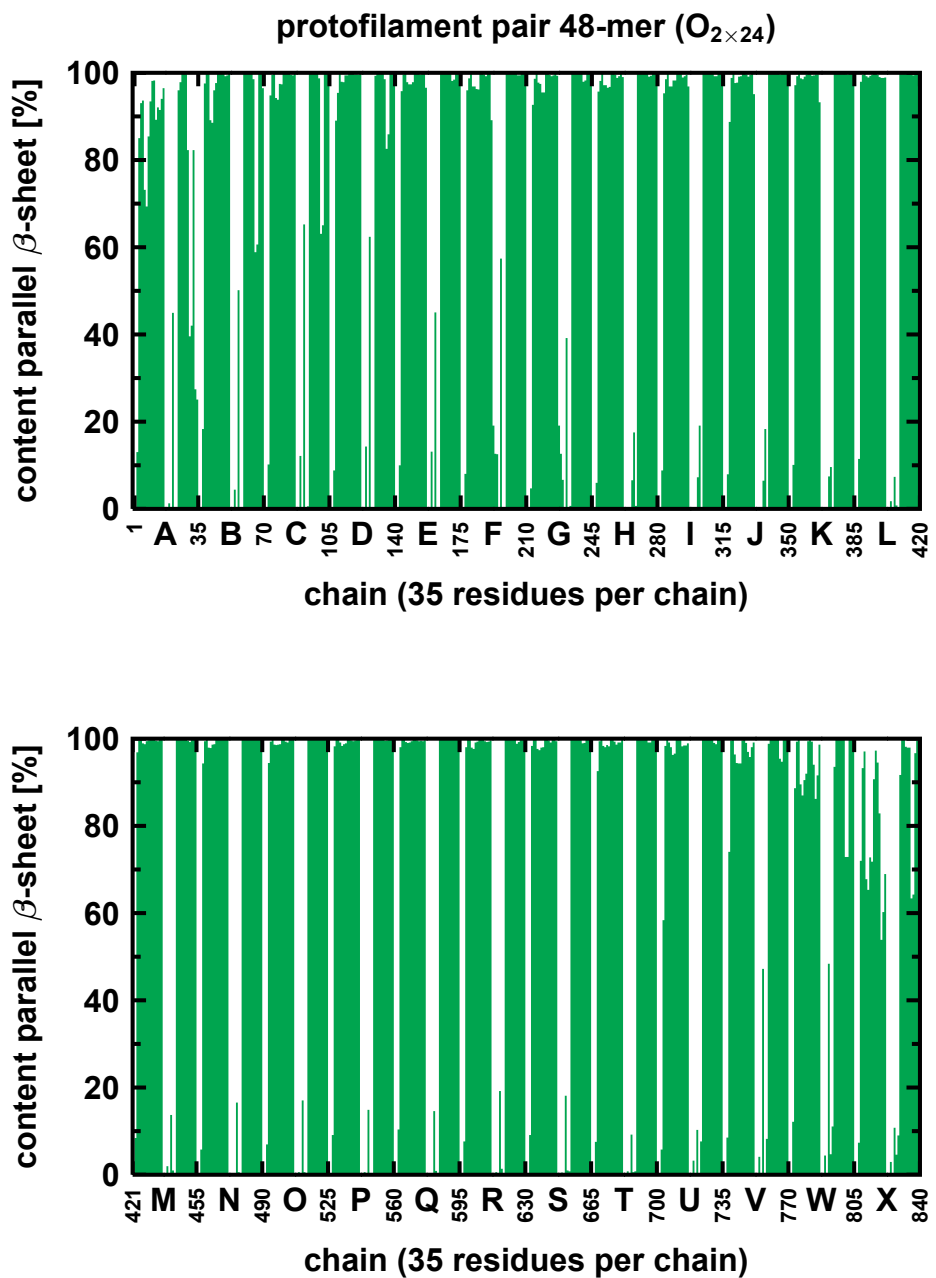


**Figure S21.** Content of parallel  $\beta$ -sheet for the large protofilament pair  $O_{2 \times 24}$ . Depicted are the first 24 A $\beta$  chains.

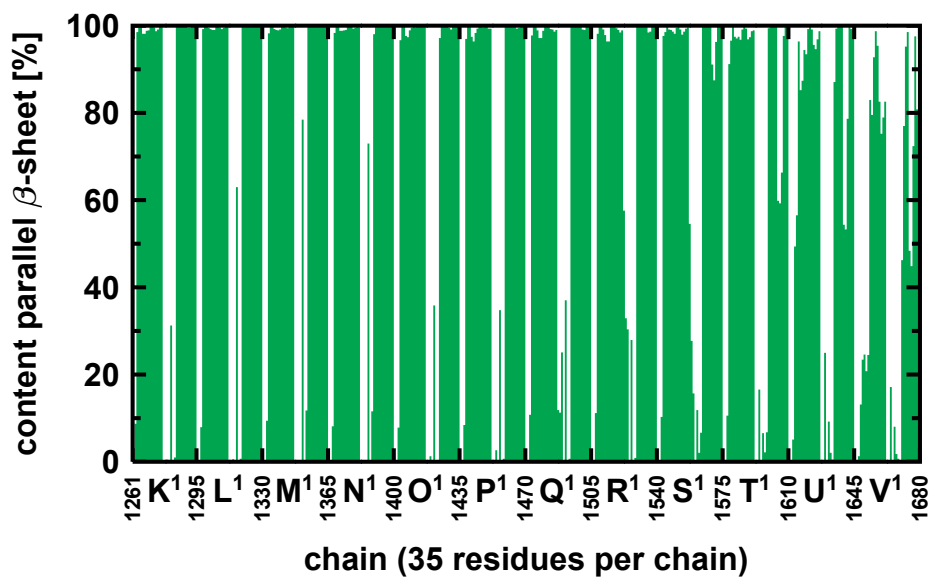
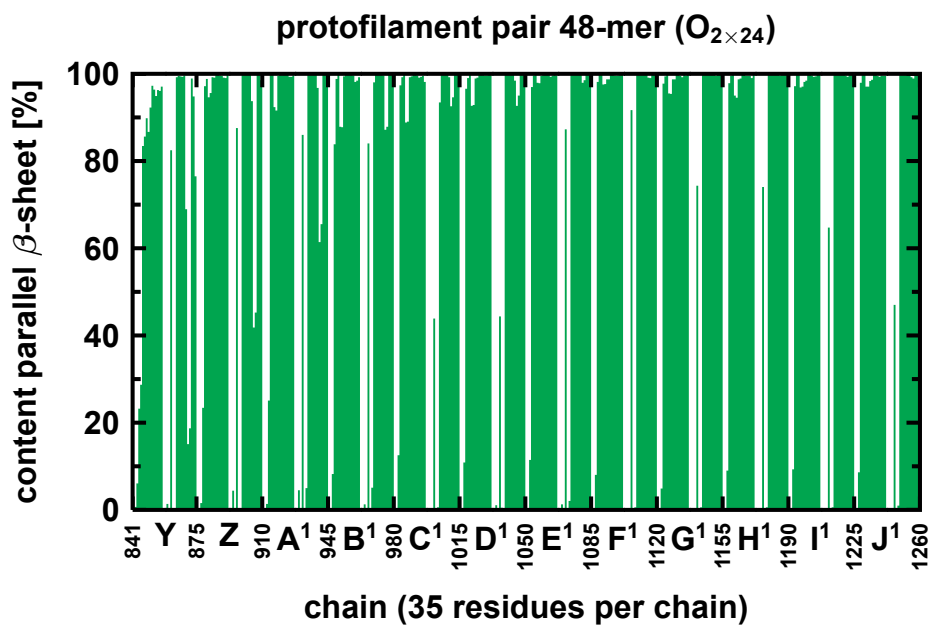


**Figure S22.** Content of parallel  $\beta$ -sheet for the large oligomer  $O_{2 \times 24}$ . Depicted are the last 24 A $\beta$  chains.

**Table S1. Appearance of inter- and intramolecular salt bridges (in %) in the MD simulation.** Each salt bridge between D23 and K28 has two distances due to the rotation of the carboxylic group of D23; OD1 and OD2 are the two oxygen atoms of the carboxylic group. Electrostatic interaction cutoff distance = 4.2 Å.

	intermolecular chains			intramolecular chain			intermolecular chains			intramolecular chain			
	OD1	OD2		OD1	OD2		OD1	OD2		OD1	OD2		
<b>O<sub>4</sub></b>	AB	81.10	83.35	A	48.38	46.23							
	BC	93.05	94.61	B	91.09	59.75							
	CD	76.79	77.08	C	90.50	75.22							
				D	50.24	50.34							
<b>O<sub>5</sub></b>	AB	92.46	90.30	A	22.53	22.53							
	BC	84.43	54.46	B	89.23	86.97							
	CD	62.00	56.81	C	80.41	76.30							
	DE	21.65	19.98	D	89.32	91.67							
<b>O<sub>6</sub></b>				E	85.70	86.29							
	AB	86.29	88.44	A	27.13	24.49							
	BC	94.91	96.87	B	45.74	60.43							
	CD	87.27	87.37	C	81.39	80.41							
	DE	64.64	64.84	D	90.30	84.04							
<b>O<sub>8</sub></b>	EF	19.78	20.67	E	77.86	79.04							
				F	78.75	80.61							
	AB	81.49	74.05	A	60.43	52.40	O <sub>2×4</sub>	AB	98.14	97.85	A	42.51	47.60
	BC	99.41	98.24	B	89.62	55.04		BC	95.69	96.77	B	81.00	70.71
	CD	91.38	91.28	C	89.32	79.92		CD	97.85	97.16	C	83.55	85.41
	DE	57.49	55.04	D	83.45	92.46					D	74.53	44.66
	EF	19.20	17.04	E	93.63	93.73		EF	87.95	88.74	E	20.76	32.03
	FG	11.07	11.75	F	96.87	94.52		FG	99.31	97.16	F	77.96	56.42
<b>O<sub>10</sub></b>	GH	13.22	13.91	G	95.10	93.93		GH	44.66	44.66	G	79.04	78.55
				H	90.21	90.01					H	71.99	67.09
	AB	84.04	86.88	A	34.87	50.05	O <sub>2×5</sub>	AB	11.36	12.24	A	13.81	16.45
	BC	84.04	84.62	B	60.14	64.25		BC	94.22	93.14	B	34.48	43.58
	CD	97.26	96.57	C	63.27	73.26		CD	96.67	95.10	C	82.76	85.11
	DE	85.41	80.12	D	78.84	83.25		DE	8.42	8.13	D	76.49	79.43
	EF	39.57	100.00	E	98.82	36.83					E	22.14	21.94
<b>O<sub>12</sub></b>	FG	98.92	99.71	F	43.78	82.76		FG	84.04	80.71	F	13.12	16.06
	GH	98.04	98.53	G	86.78	86.39		GH	96.18	97.45	G	46.82	80.31
	HI	98.73	97.55	H	73.75	93.05		HI	67.78	68.36	H	94.61	71.79
	IJ	48.09	47.40	I	70.91	91.09		IJ	48.48	47.89	I	91.09	95.89
				J	80.90	80.71					J	83.35	77.47
	AB	86.78	93.44	A	44.27	31.44	O <sub>2×6</sub>	AB	92.85	90.99	A	47.80	38.59
	BC	91.19	96.18	B	47.11	43.29		BC	100.00	99.22	B	85.01	88.25
	CD	97.75	97.36	C	77.47	71.01		CD	67.29	68.36	C	90.99	90.99
	DE	98.53	96.77	D	73.95	67.78		DE	59.16	57.49	D	89.03	93.63
	EF	96.28	96.87	E	73.75	80.71		EF	11.46	11.66	E	90.79	90.60
<b>O<sub>24</sub></b>	FG	95.49	94.91	F	70.52	76.00					F	74.44	71.11
	GH	74.63	75.32	G	78.94	56.42		GH	56.42	73.26	G	68.46	65.33
	HI	19.10	18.81	H	67.48	73.95		HI	72.77	69.83	H	63.08	70.03
	IJ	89.13	89.91	I	32.13	34.08		IJ	37.32	38.59	I	92.07	92.26
	JK	96.67	97.94	J	45.84	31.64		JK	26.25	27.72	J	96.47	90.11
	KL	99.12	98.82	K	76.10	82.57		KL	12.24	12.14	K	89.52	89.62
				L	64.25	66.11					L	25.47	22.14
	AB	96.28	94.71	A	54.36	61.80	O <sub>2×12</sub>	AB	83.25	80.71	A	53.97	52.01
	BC	99.02	98.53	B	90.99	86.29		BC	97.36	98.73	B	76.69	91.38
	CD	97.26	93.54	C	85.01	86.19		CD	99.90	99.02	C	90.70	90.99
<b>O<sub>24</sub></b>	DE	87.86	89.03	D	80.80	82.76		DE	99.02	98.92	D	92.85	75.02
	EF	90.50	92.56	E	81.98	81.98		EF	98.92	99.12	E	96.67	88.54
	FG	85.99	85.21	F	79.24	73.85		FG	96.57	96.18	F	90.11	90.70
	GH	63.76	61.31	G	68.17	78.45		GH	99.80	99.12	G	85.60	84.13
	HI	11.85	10.58	H	65.43	65.92		HI	99.71	99.80	H	82.57	86.19
	IJ	96.87	95.20	I	87.86	88.54		IJ	99.41	99.80	I	81.88	86.48
	JK	98.92	99.61	J	87.86	77.57		JK	99.22	99.22	J	60.82	81.98
	KL	99.71	99.80	K	88.25	90.79		KL	3.23	3.33	K	82.57	79.04
	LM	77.18	61.61	L	37.22	87.27					L	14.79	14.89

Continued on Next Page...

Table S1 – Continued

intermolecular chains		intramolecular chain		intermolecular chains		intramolecular chain							
	OD1	OD2		OD1	OD2		OD1	OD2					
	MN	93.24	89.62	M	87.66	92.46	MN	79.53	80.90	M	59.84	64.05	
	NO	98.04	97.16	N	93.34	92.46	NO	88.93	93.63	N	88.93	85.90	
	OP	96.67	95.49	O	93.63	96.18	OP	94.22	96.28	O	85.41	87.66	
	PQ	99.90	99.80	P	91.87	91.19	PQ	99.71	99.02	P	70.32	70.62	
	QR	93.24	99.71	Q	86.97	96.38	QR	98.53	98.04	Q	86.19	93.14	
	RS	45.15	44.96	R	69.44	69.64	RS	98.73	99.41	R	84.92	85.50	
	ST	37.22	38.49	S	92.07	94.22	ST	99.90	99.71	S	74.73	73.95	
	TU	15.67	15.28	T	94.91	95.79	TU	99.51	99.90	T	60.43	81.49	
	UV	12.54	12.44	U	95.59	95.79	UV	98.14	98.24	U	83.25	90.60	
	VW	11.17	11.17	V	97.16	95.59	VW	73.75	75.81	V	75.22	67.09	
	WX	9.21	9.30	W	76.20	89.72	WX	78.45	78.75	W	51.91	50.73	
			X	25.66	27.23				X	65.52	70.03		
O <sub>48</sub>	AB	96.08	93.14	A	58.08	64.25	O <sub>2×24</sub>	AB	84.33	85.41	A	51.32	51.32
	BC	90.30	68.66	B	87.27	92.26		BC	99.31	99.51	B	83.15	88.74
	CD	91.48	92.36	C	83.64	84.62		CD	98.73	99.22	C	94.12	95.89
	DE	98.92	98.82	D	68.76	78.84		DE	86.97	80.41	D	78.65	79.53
	EF	88.15	82.86	E	63.47	70.23		EF	96.77	96.67	E	54.95	72.58
	FG	78.45	48.19	F	31.34	43.88		FG	85.99	81.88	F	87.27	92.07
	GH	99.12	99.71	G	85.01	59.84		GH	99.12	99.22	G	63.76	60.92
	HI	99.31	98.82	H	85.11	86.09		HI	99.90	99.51	H	62.10	80.90
	IJ	96.87	90.89	I	71.30	84.23		IJ	100.00	99.71	I	82.47	85.11
	JK	99.31	100.00	J	91.87	94.52		JK	100.00	99.90	J	55.63	94.71
	KL	100.00	99.90	K	69.93	88.34		KL	96.08	94.52	K	75.61	74.14
	LM	99.61	97.36	L	59.45	92.26		LM	98.73	98.92	L	71.50	74.44
	MN	99.61	100.00	M	98.14	89.32		MN	99.80	99.71	M	76.79	78.06
	NO	100.00	100.00	N	85.01	93.24		NO	99.80	100.00	N	80.90	82.96
	OP	34.77	42.70	O	64.64	55.14		OP	99.80	99.90	O	80.80	84.33
	PQ	96.47	97.16	P	90.99	82.86		PQ	100.00	100.00	P	64.54	77.08
	QR	99.90	99.51	Q	93.05	92.75		QR	99.51	99.90	Q	90.01	74.63
	RS	98.82	96.77	R	86.88	95.40		RS	99.31	99.41	R	58.18	88.74
	ST	91.38	95.10	S	85.80	94.03		ST	99.71	99.22	S	69.64	93.83
	TU	98.92	99.71	T	32.71	84.62		TU	70.71	69.15	T	78.75	83.35
	UV	36.14	87.66	U	95.20	94.22		UV	54.06	54.75	U	87.07	82.76
	VW	77.18	74.63	V	73.26	75.61		VW	54.26	53.48	V	90.21	87.76
	WX	100.00	99.90	W	87.07	96.77		WX	8.23	9.21	W	86.19	87.37
	XY	77.18	87.76	X	90.79	22.53				X	67.19	66.90	
	YZ	86.19	91.48	Y	76.00	57.79		YZ	92.36	53.67	Y	42.51	63.27
	Z <sup>A</sup> <sup>1</sup>	89.91	95.79	Z	96.87	90.70		Z <sup>A</sup> <sup>1</sup>	99.61	99.80	Z	85.21	92.95
	A <sup>1</sup> B <sup>1</sup>	98.73	98.73	A <sup>1</sup>	76.98	43.88		A <sup>1</sup> B <sup>1</sup>	99.61	99.90	A <sup>1</sup>	88.25	90.99
	B <sup>1</sup> C <sup>1</sup>	45.74	48.48	B <sup>1</sup>	78.06	46.72		B <sup>1</sup> C <sup>1</sup>	77.18	75.81	B <sup>1</sup>	79.43	76.10
	C <sup>1</sup> D <sup>1</sup>	95.40	95.40	C <sup>1</sup>	90.40	90.30		C <sup>1</sup> D <sup>1</sup>	57.49	59.26	C <sup>1</sup>	66.90	70.81
	D <sup>1</sup> E <sup>1</sup>	100.00	100.00	D <sup>1</sup>	91.09	87.95		D <sup>1</sup> E <sup>1</sup>	97.45	97.26	D <sup>1</sup>	44.27	76.30
	E <sup>1</sup> F <sup>1</sup>	99.22	99.22	E <sup>1</sup>	92.65	95.98		E <sup>1</sup> F <sup>1</sup>	99.22	99.41	E <sup>1</sup>	84.04	90.11
	F <sup>1</sup> G <sup>1</sup>	100.00	100.00	F <sup>1</sup>	90.79	88.93		F <sup>1</sup> G <sup>1</sup>	99.90	99.71	F <sup>1</sup>	65.43	91.87
	G <sup>1</sup> H <sup>1</sup>	99.90	99.61	G <sup>1</sup>	85.21	87.27		G <sup>1</sup> H <sup>1</sup>	99.22	99.90	G <sup>1</sup>	89.72	85.90
	H <sup>1</sup> I <sup>1</sup>	75.91	81.59	H <sup>1</sup>	80.80	65.82		H <sup>1</sup> I <sup>1</sup>	99.80	98.33	H <sup>1</sup>	76.59	83.55
	I <sup>1</sup> J <sup>1</sup>	45.35	46.13	I <sup>1</sup>	94.81	88.74		I <sup>1</sup> J <sup>1</sup>	99.51	99.31	I <sup>1</sup>	72.48	76.69
	J <sup>1</sup> K <sup>1</sup>	14.10	10.48	J <sup>1</sup>	67.78	79.63		J <sup>1</sup> K <sup>1</sup>	99.51	98.82	J <sup>1</sup>	83.64	79.24
	K <sup>1</sup> L <sup>1</sup>	63.17	75.51	K <sup>1</sup>	91.28	88.15		K <sup>1</sup> L <sup>1</sup>	99.90	99.71	K <sup>1</sup>	86.29	85.31
	L <sup>1</sup> M <sup>1</sup>	88.74	87.66	L <sup>1</sup>	80.90	84.92		L <sup>1</sup> M <sup>1</sup>	99.90	99.90	L <sup>1</sup>	60.04	81.68
	M <sup>1</sup> N <sup>1</sup>	99.02	99.41	M <sup>1</sup>	87.46	90.40		M <sup>1</sup> N <sup>1</sup>	99.90	99.61	M <sup>1</sup>	49.07	99.02
	N <sup>1</sup> O <sup>1</sup>	99.02	99.22	N <sup>1</sup>	92.85	87.66		N <sup>1</sup> O <sup>1</sup>	99.80	100.00	N <sup>1</sup>	85.50	71.50
	O <sup>1</sup> P <sup>1</sup>	61.51	53.28	O <sup>1</sup>	50.24	82.66		O <sup>1</sup> P <sup>1</sup>	99.90	99.80	O <sup>1</sup>	87.07	61.70
	P <sup>1</sup> Q <sup>1</sup>	39.67	37.22	P <sup>1</sup>	89.62	91.67		P <sup>1</sup> Q <sup>1</sup>	99.61	99.90	P <sup>1</sup>	82.47	87.76
	Q <sup>1</sup> R <sup>1</sup>	54.75	62.88	Q <sup>1</sup>	90.50	90.01		Q <sup>1</sup> R <sup>1</sup>	91.87	89.91	Q <sup>1</sup>	64.64	70.13
	R <sup>1</sup> S <sup>1</sup>	98.92	99.12	R <sup>1</sup>	57.00	54.85		R <sup>1</sup> S <sup>1</sup>	94.61	96.38	R <sup>1</sup>	50.24	51.71
	S <sup>1</sup> T <sup>1</sup>	94.61	95.10	S <sup>1</sup>	88.54	87.95		S <sup>1</sup> T <sup>1</sup>	58.57	55.04	S <sup>1</sup>	68.36	74.44
	T <sup>1</sup> U <sup>1</sup>	56.32	55.04	T <sup>1</sup>	87.56	88.93		T <sup>1</sup> U <sup>1</sup>	27.91	29.77	T <sup>1</sup>	84.04	77.86
	U <sup>1</sup> V <sup>1</sup>	41.04	41.82	U <sup>1</sup>	92.95	90.60		U <sup>1</sup> V <sup>1</sup>	10.19	8.81	U <sup>1</sup>	94.03	94.71
			V <sup>1</sup>	76.30	74.73					V <sup>1</sup>	79.14	87.56	